



Tomas Bata University in Zlín
Library

Optimal cutting parameter specification of newly designed milling tools based on the frequency monitoring

Citation

MONKA, Peter Pavol, Katarína MONKOVÁ, Vidoslav D. MAJSTOROVIĆ, Željko BOŽIĆ, and Andrej ANDREJ. Optimal cutting parameter specification of newly designed milling tools based on the frequency monitoring. *International Journal of Advanced Manufacturing Technology* [online]. Springer Science and Business Media Deutschland, 2020, [cit. 2023-02-06]. ISSN 0268-3768. Available at <https://link.springer.com/article/10.1007/s00170-020-06169-x>

DOI

<https://doi.org/10.1007/s00170-020-06169-x>

Permanent link

<https://publikace.k.utb.cz/handle/10563/1010010>

This document is the Accepted Manuscript version of the article that can be shared via institutional repository.



TBU Publications

Repository of TBU Publications

publikace.k.utb.cz

Optimal cutting parameter specification of newly designed milling tools based on the frequency monitoring

Peter Pavol Monka^{1,2} • Katarina Monkova^{1,2} • Vidosav D. Majstorovic³ • Željko Božić⁴ • Andrej Andrej¹

¹ Faculty of Manufacturing Technologies with the Seat in Presov, Technical University in Kosice, Presov, Slovakia

² Faculty of Technology, Tomas Bata University in Zlin, Zlin, Czech Republic

³ Faculty of Mechanical Engineering, University of Belgrade, Belgrade, Serbia

⁴ Faculty of Mechanical Engineering and Naval Architecture, University of Zagreb, Zagreb, Croatia

* Katarina Monkova katarina.monkova@tuke.sk, Vidosav D. Majstorovic vidosav.majstorovic@sbb.rs, Željko Božić Zeljko.Bozic@fsb.hr, Andrej Andrej andrej2x@gmail.com

Abstract

The article deals with the specification of the most suitable machining parameters for three newly designed end mills in the term of stability of the deep groove machining, at which the depth of cut is minimally twice higher the diameter of the cutter. Online vibration analysis was selected as a tool for goal achievement. The partial objective of the first phase of experimental research was to set the boundary conditions of vibrodiagnostics at the specification of the behaviour of three commercially produced milling cutters when the results were compared with the surface roughness achieved at the machining with individual cutting parameters. Vibrodiagnostic conditions were subsequently applied in the second phase of the experiment to determine the most suitable machining parameters of newly designed milling cutters. The Pinnacle VMC 650 CNC machining centre with Fanuc control system was used to perform the experiments. The material of cutters was S-grade sintered carbide, and all the designed cutters were PVD coated with the same AlTiN (aluminium titanium nitride) coating. The machined material was 16MnCr5 (1.7131) steel. The surface roughness analysis after machining by newly designed cutters pointed out that they are better as for the surface quality in comparison with the commercially produced end mills. Finally, it was possible to state that the four-tooth cutter 01-FVT with helix angles ($\beta_1 = 39^\circ$ and $\beta_2 = 41^\circ$) and tooth pitch ($\tau_1 = 83^\circ$ and $\tau_2 = 97^\circ$) seems to be the best tool for milling deepshaped grooves among all the tested milling cutters.

Keywords: Mill cutter, Tool geometry, Deep groove, Vibrations monitoring, Cutting parameters

Nomenclature

f_n	Feed per revolution (mm/rev)
f_z	Feed per tooth (mm)
v_c	Cutting speed (m/min)
a_p	Depth of cut (mm)
γ	Rake angle ($^\circ$)
β	Helix lead angle ($^\circ$)
τ	Pitch angle of teeth ($^\circ$)
D	Diameter of milling cutter (mm)
R_a	Arithmetical average deviation from a mean line (μm)
R_z	Maximal height of profile irregularities (μm)
PVD	Physical vapour deposition
FEM	Finite element method
RMS	Root mean square
FFT	Fast Fourier transformation
CNC	Computer numerical control
CF	Crest factor
VQMHVD	Type of commercially produced milling cutter
HHW	Type of commercially produced milling cutter

1 Introduction

Along with the automation of manufacturing systems, currently, machining process control becomes an essential issue in machining operations to carry out the manufacturing processes efficiently, smoothly and safely, especially in today's unmanned machining systems. However, many current manufacturing trends such as the demand for high-quality workpieces, new materials that are more difficult to machine, requirements for reducing tolerances or increasing reliable repeatability increase the burden on machining systems.

On the other hand, to save time and money, manufacturers consolidate multiple parts into one-piece monolithic workpieces that require the machining of deep holes and cavities of complex components on machine tools capable of performing multiple tasks simultaneously. Such milling can result in tool misalignment. It can cause vibrations and shakiness that reduce the surface quality of the parts, cause rapid wear or breakage of cutting tools and damage machine tool components, requiring costly repairs and longer downtime [1]. The varying forces result in the imbalance of machine components, insufficient system rigidity, or resonant vibration of machine tool elements. Cutting pressures are also changing as the tool periodically loads and releases the wedge when chipping and chip breaking [2].

However, current trends are moving towards an unattended system, which requires that the system would be stable, resp. to be possible to stabilize it. Manufacturers seeking to overcome these problems need to analyse all the elements of their machining systems and use methods and tools to guarantee their success. One of the basic ways of ensuring a stable and reliable operation is the monitoring of the machining process. By implementing sensors in machining centres, it is possible today to monitor the engine power, cutting force, tool and workpiece temperature changes, torque, chip shaping and breakage, tool damage, surface quality, system shaking, etc. The signals from the individual sensors provide important information, either for control or for diagnostics a problem in the machining process [3, 4]. Based on the knowledge of the behaviour of individual elements of the system, it is then possible to eliminate the deficiencies of the machining system as a whole and to achieve maximum productivity and profitability. It also leads to the balancing of many factors affecting the production process, which lead to the elimination (or minimization) of vibration and thus to ensure the desired product quality.

After a brief overview of the current state in the topics covered in the manuscript, “**Materials, methods and equipment**” section presents the cutters, methods, equipment and conditions of the experiments that were used in the research. The following “**Results and discussions**” section is divided into two parts, where the first part presents an evaluation of the vibration behaviour of commercially produced end mills to determine the boundary conditions of the main experiments (carried out in the second phase), in which the newly designed end mills were evaluated to specify the best technological parameters of machining with these milling cutters. The achieved results are described and discussed in this section, and they are also summarized in the “**Conclusions**”.

2 State of the art

Nowadays, when engineering production reaches almost all branches of industry and when products contain increasingly complex shapes, it is often necessary to create different cavities, holes or grooves of small diameters and large depths. Milling in which the depth of cut is at least $2xD$ compared with its diameter (D is the diameter of the milling cutter) is mainly used in the production of complex moulds for injection moulding, machining of functional surfaces of die casting or milling of deep grooves for various purposes, e.g. when machining gears for chain transmissions etc. Milling with large tool offsets is generally a problem that often causes unwanted tool shaking, which affects not only the stability of the machine-tool-workpiece system but especially the quality of the machined surface.

The stability of the cutting process is a complex problem that is affected not only by cutting parameters (chip thickness and width, cutting speed and feed) [5, 6], but also by geometry and shape of the tool's cutting wedge [7, 8] and, to a lesser extent, a tool wear itself [9]. It should be noted, however, that these various aspects are closely related and influence each other.

The effect of cutting conditions on the stability of the cutting tool, or the cutting process itself, is most closely related to changing the size and direction of the cutting forces [10, 11]. The intensity of their influence is also given by the properties of the machine-tool-workpiece system, their stiffness, damping constants, resonant frequencies and so on.

The first step to reducing vibration during tool milling is to select the correct geometry and number of cutting wedges. Based on [12, 13], it can be said that the use of fewer teeth results in partial vibration damping. Properly designed size and shape of the tooth gap is also an important factor in reducing frequencies during milling. Its determination is based mainly on the shape and size of the cross section of the material layer to be removed, the shape of the resulting chip and, last but not least, its volume coefficient [14, 15]. The next studies [16-18] describe that tools with uneven tooth pitch or different

helix angles have a positive effect on-chip thickness, thus eliminating the occurrence of a regenerative effect.

Kim [19] defined the basic steps of milling cutters grinding and points out the methods of cutting wedge modifications. The detailed model processed by the author can be used in various simulations, FEM analyses, or mathematical verifications. Concerning the shape of the cutting wedge, researchers in their studies [20-22] show that positive geometry reduces cutting forces by up to 20% compared with zero or negative geometry. Takuya [23] have mentioned that a greater helix angle causes less harmonic oscillation and also that for smaller vibrations, it is better to use a milling cutter diameter 20 to 50% greater than the cut width taken.

The problem of correct design of the cutting wedge and the shape of a tool face to reduce vibration, including the increasing the stability of the milling cutter, was discussed by several researchers. Grabowski [24] deals with the topic of cutting force prediction and increasing the stability of milling cutters in the machining process by changing a cutter geometry. The main essence of the tools examined in his study was to reduce cutting forces by using a serrated cutting edge, uneven tooth pitch and helix pitch, resulting in the elimination of vibration during machining.

During the machining of material by such milling cutters, there is a variable change in the thickness of the cut-off material layer, while the author describes this change as the static $h_{stat, j, u}(z)$ and dynamic $h_{dyn, j, u}(z)$ component of the chip by relation (1) [24].

$$h_{stat, j, u}(z) = f(z) \sin(\varphi_j(z)) + r_j(z) - r_u(z) \quad (1)$$

where $f(z)$ is the feed per tooth, j is the angular rotation of the j th tooth, $\varphi_j(z)$ is the chip width at the j th angular rotation, $r_j(z)$ is the radius of the j th tooth along the z -axis and $r_u(z)$ is the radius of the u th tooth along the z -axis.

Feed per tooth $f(z)$ is constant; however, uneven tooth pitches and helix lead to cause the thickness of the cut layer during engagement of the j tooth to be greater (or smaller) compared with the thickness when $u = j + 1$ tooth works. This phenomenon is described by relation (2) [24].

$$f_{j, u}(z) = f(z) N_t \frac{p_{j, u}(z)}{2\pi}, \quad (2)$$

where N_t is the total helix height and $p_{j, u}(z)$ is the helix angle between j and u teeth.

The used distribution of the teeth is shown in Fig. 1, wherein the j th tooth is designated as $j = 1$. Then, the lead angle $p_{j, u}(z)$ can be defined as (3):

$$p_{j, u}(z) = 2\pi + \varphi_u(z) - \varphi_j(z) - 2\pi \left[\frac{\varphi_u(z) - \varphi_j(z)}{2\pi} \right] \quad (3)$$

A dynamic component of a removed layer $h_{\text{dyn},j,u}(t, z)$ is specified by Eq. (4):

$$h_{\text{dyn},j,u}(z) = \Delta n_j(t - \theta_{j,u}(z)) - \Delta n_j(t) \quad (4)$$

where $\Delta n_j(t)$ represents the relative displacement between a tool and a workpiece and $\Delta n_j(t - \theta_{j,u}(z))$ represents a dynamic displacement of the surface undulated after the previous tooth.

Similarly, like the thickness of the cut-off layer in the static component $f_{j,u}(z)$, the dynamic component $\theta_{j,u}(z)$ is also described in the following dependency (5) [24, 25]:

$$\theta_{j,u}(z) = n \frac{p_{j,u}(z)}{2\pi} \quad (5)$$

where n is a spindle speed.

Wan [25] has experimentally verified that wear affects the change in cutting force in such a way that the feed and passive forces are more influenced by tool wear than the cutting force. It is further reported in his study that if there is an increase in wear on the clearance angle, the contact area increases and also the amplitude of the dynamic force oscillations increases, which leads to a reducing the stability of the cutting tool.

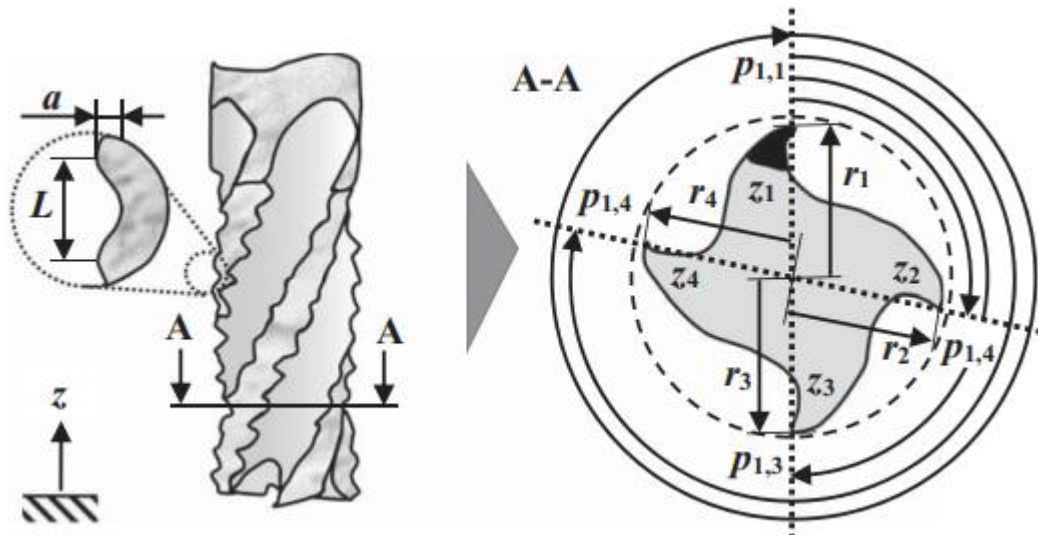


Fig. 1 Teeth distribution [24]

The topic of correct design of the cutting wedge and the shape of the face, for the best chip removal, which would result in reduced vibration, respectively in increasing the stability of the cutter, was dealt with by Subramanian [26]. He defined the basic procedures for grinding milling cutters and pointed

out the methods of the cutting wedge modification by means so-called a detailed model that can be used in various simulations using FEM (finite element method) or mathematical variations of the next modifications.

The studies [27-29] deals with the prediction of tool stability in terms of vibration. He defines the basic mathematical model for the oscillating system and provides a brief overview of the workflow, using a method of vibrational deformations of the movement of the tool based on time records solved from the simulation.

The cutting properties of the workpiece material such as material hardness, susceptibility to the built-up edge creating or to a strain hardening, respectively the presence of hard inclusions, may contribute to vibrations. These sources of vibration cause process instability or resonance, which also synchronizes with the natural spindle frequency of the machine or the natural frequency of the tool, resulting in unwanted vibrations. Variable cutting forces during chip's formation and breakage become an additional source of vibration that can resonate along with the natural vibration mode of the tool holder or machine tool and so to maintain or even increase the amplitude of oscillation [30-32].

The material, type of finishing and shape of the end mills are key factors for improving cutting performance, where the shape and design of the milling cutters primarily affect machining accuracy and dynamic stability. Therefore, in solving problems with tool stability in milling, where the depth of cut is greater than $2 \times D$, the authors focused on adjusting the geometry and shape of the milling cutter. Preliminary research resulted in the design, construction and production of 3 new end milling cutters intended for milling deep grooves.

The principal objective of the article was to specify the most suitable machining parameters (cutting speed and depth of cut) for three newly designed end mills in the term of stability of the deep grooves machining, at which the depth of cut is minimally twice higher the diameter of the cutter. The online vibration analysis was selected as a tool for goal achievement. Based on the overview of the scientific literature and based on the State of the art above it can be said that in recent years the vibrodiagnostics is used in machining process not only because of monitoring good conditions of a machine but still more often also for the identification of tool wear when the geometry of cutting wedge and cutting conditions have been already selected. However, based on the best knowledge of the authors, the vibrodiagnostics has not been yet used in the opposite way to find the best cutting conditions and the cutting tip geometry for milling cutter. So, as a novelty of the research can be considered the identification of the most suitable machining parameters of newly designed cutters using the vibration analysis and mathematical description of the end mills behaviour expressed by the dependency of RMS (root mean square) values on the cutting speed and depth of cut. Authors suggested a methodology for selection of the most appropriate cutting conditions, while they designed the groove type consisting of four sectors that represent the basic trajectories of the cutter during a groove machining generally and they also designed the evaluation procedure at "a midpoint" of every sector of the groove using RMS technique. To confirm the approach and to set up properly the boundary conditions for vibrodiagnostics employed within the primary goal fulfilment, the monitoring of the behaviour of three commercially produced milling cutters through vibrodiagnostics was selected as the partial objective while the obtained results were compared with the surface roughness achieved at the machining with individual cutting parameters. It was confirmed that with tool wear increasing, the surface roughness increases what also corresponded with higher vibrations that have been measured.

Since the development of new materials intensively continues, it brings new challenges also for new tool materials and so for the new tools' geometries set-up. The approach based on experimental methodology presented in the study, connected with the numerical simulation in preliminary research,

can be applied for all machining tools and can bring not only faster solution but it can have also economic benefits.

3 Materials, methods and equipment

3.1 Experimental tools




3.1.1 Commercially produced milling cutters

In the first phase of the experiment, three commercially produced milling cutters were used. All these end mills are from sintered carbide, but they have different helix leads and different coatings. End mill “VQMHVD” is a vibration-damping cutter for machining hard-to-machine materials.

End mill “HHW” is a universal cutter for roughing or smoothing, with very quiet running due to uneven teeth distribution, with blade protection for longer durability and maximum runout of 0.01 mm. End mill “HHW BlueCut” is a high-performance cutter with dynamic torque (40°) for a high machining performance and with a high wear resistance due to nanocomposite coating. The shape of the groove ensures good chip removal, quiet running during roughing and smoothing.

The commercially produced milling cutters used within the research are shown in Table 1, where also the basic characteristics are presented.

Table 1 Basic characteristics of commercially produced milling cutter

		VQMHVD 1000	HHW 97.016.809	HHW BlueCut 98.102.028
Indication				
Producer		Mitsubishi	Hommel Hercules Werkzeughandel	Hommel Hercules Werkzeughandel
Diameter ϕD (mm)		10	10	10
Number of teeth		4	4	4
Maximum cutting depth a_p (mm)		22	22	22
Length L (mm)		70	72	72
Helix lead β_1 (°)		37	35	40
Helix lead β_2 (°)		40	38	-
Pitch angle of teeth τ_1 (°)		85	85	85
Pitch angle of teeth τ_2 (°)		95	95	95
Coating	Type	AlCrN	TiAlN	NaCo
	Coating hardness (HV)	3200	2800	4500
	Maximal working temperature of coating (°C)	1100	700	1200
	The friction coefficient of coating relative to steel	0.35	0.6	0.45

3.1.2 Newly designed milling cutters

In the second phase of the experiment, several variations of special milling cutters were designed by the authors. In the preparatory phase of the research, the milling cutters were modelled in Solid Edge® software, and their machining behaviour was simulated in Simulia-ABAQUS® using the FEM. The method assisted to design a tool geometry, to evaluate the cutter behaviour at machining and to improve its geometry by minimizing von Mises stress [33, 34].

The numerical method used in the study included the following steps: the material constitutive model definition, fracture criterion and characteristics of contact friction and equation of heat conduction. Within the first step, Johnson-Cook model was used that is usually is used to describe under the condition of the large deformation, high strain rate effect and temperature, especially the model is widely used in the transient and dynamic simulation. The second step was based on the rupture equation using the rule of Johnson-Cook's shear failure to make the cutting the element material taking place of failure in the process of simulation of cutting. A friction model was proposed according to Zorev [35] so the contact area of the tool and workpiece has two different contact state, namely the sliding zone and the bond zone. The shear stress at every point in the bonding zone is the basic same; friction stress in the sliding area decreases with a cutting tool rake angle, and meet the Coulomb law of friction assuming a friction coefficient of 0.3. The analysis considers the heat generated by plastic straining of the material by using inelastic heat fraction option available in ABAQUS®. For all simulations with the goal to narrow down the selection of designed milling cutters, the same characteristics of both tool and workpiece materials were applied which were S-grade sintered carbide and 16MnCr5 steel respectively. The cutting tool was set to the rigid body within the research. For the mesh creation, the C3D8RT element type was selected with a total number of 108,244 elements with 115,287 nodes while the mesh was finer in the contact zone.

The results of the simulation helped authors to reduce the number of variants of the proposed milling cutters and proceed to the production of only the most suitable prototypes. An example of the diagrams showing the simulation results related to von Mises stress courses for the cutters with 3 and 4 teeth is in Fig. 2.

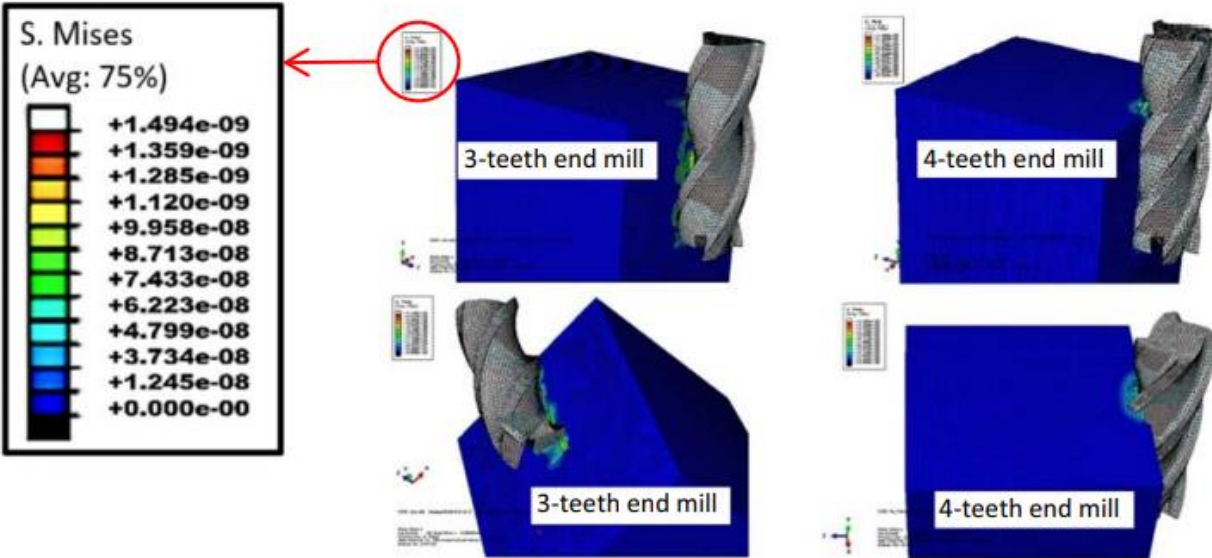


Fig. 2 Pictures from the partial simulations in software Simulia-ABAQUS®

Three appropriate end mills were selected, namely milling cutters labelled 01-FVT, 02-FVT and 03-FVT, for the real production and testing. The basis of all three variants of the newly designed tools was a milling cutter with a diameter $D = 10$ mm, a working length of 40 mm and a total length $L = 100$ mm. The cutting wedge and its face with a rake angle $\gamma = 10^\circ$ were shaped for optimum chip removal. The cutters differ in the number of teeth and helix angles. The basic sizes and angles of a cutting wedge are shown in Fig. 3.

The material of cutters is S-grade sintered carbide and all the designed cutters were PVD coated with the same “Eifeler Extral” coating. It is an AlTiN (aluminium titanium nitride) coating, specially designed for heavy dry applications under extreme conditions. It is also intended for milling the steels with hardness above 50 HRC. It is characterized by high oxidation resistance (800 °C), high heat hardness, low thermal conduction coefficient and high resistance to chemical influences. The basic characteristics of the designed end mills are presented in Table 2, where also the pictures of real produced cutters are provided.

3.2 Machined material

The 16MnCr5 steel (1.7131, EN 10084) was selected as a material to be machined during experiments. It is a manganese chromium steel for cementing, with a carbon content of 0.14 to 0.19 wt%, intended for a wide range of production. The steel is hot and cold deformable; it has good weldability and is most often used for parts up to $\phi 35$ mm in diameter for refinement, cementing with high core strength (e.g. shafts, gears, valve jacks, piston pins or teeth clutch). The chemical composition of the steel is shown in Table 3 [36].

The main reason for selection of this material for experimental verification of the proposed cutters was its frequent use in the production of sprockets for chain drives, where the cutter overhang is very large (the tool overhang is at least $4 \times D$, while the cutter usually has to work many times up to the depth of cut $3 \times D$).

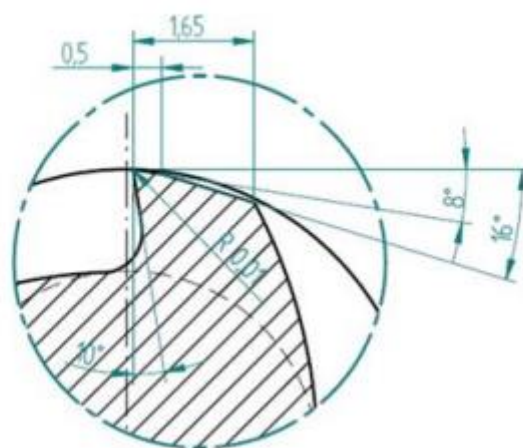





Fig. 3 Sizes and angles of a cutting wedge

Table 2 Basic characteristics of newly designed milling cutters

		01-FVT	02-FVT	03-FVT
Indication				
	Helix lead β_1 (°)	39	36	39
	Helix lead β_2 (°)	41	38	40
	Helix lead β_3 (°)	-	-	41
	Pitch angle of teeth τ_1 (°)	83	83	120
	Pitch angle of teeth τ_2 (°)	97	97	120
	Number of teeth	4	4	3
	Coating	Type	AlTiN, created by PVD technology	
Coating hardness (HV)		3300 ±300		
Maximal working temperature of coating (°C)		800		
The friction coefficient of coating relative to steel		0.7		

3.3 Conditions of the experiment

The experiment to compare and verify the stabilization of milling tools was completely realized at the authors' workplace. The machine used to carry out the experiments was a CNC machining centre of the Pinnacle VMC 650 brand with the Fanuc control system. A workpiece clamping was carried out using a machine vice; tools were clamped using a collet in a tool holder, and some cases with a hydraulic clamp of Vertex company.

As mentioned above, the material to be machined was steel with the designation 16MnCr5 steel. The sizes of the workpieces were designed so that the milled grooves and the gaps between them were not too small, due to the sufficient rigidity of the material. Each piece of the workpiece was 120 x 120 x 50 mm (± 1 mm), and three grooves with a maximum depth of 30 mm were milled per workpiece (Fig. 4 left). The groove shape has been designed specifically for experimental testing so that the groove contains the basic form elements (straight and curved), which usually the deep grooves in real practice contain. The partial grooves were defined on the workpiece as sectors I-IV. The groove width was 10 mm (related to the diameter of the milling cutters), while the lengths of the individual paths are indicated by a red line in Fig. 4 right. The total length of the groove (or tool path) was 150 mm.

An important aspect to be mentioned is the overhang of a tool from the clamping. Just the length at which the cutting tool must work affects the increase, respectively reduction, of vibration substantially. However, since all milling cutters within a group were clamped with the same overhang value (commercial milling cutters with 32-mm overhang and designed milling cutters with 45-mm overhang), this factor is taken as a constant and therefore does not affect the evaluation, as the comparison of milling cutters took place separately between commercial cutters and separately between the designed cutters.

Table 3 The chemical composition of the 16MnCr5 steel [36]

C (wt%)	Mn (wt%)	Si (wt%)	Cr (wt%)	P max. (wt%)	S max. (wt%)
0.14–0.19	1.10–1.40	0.17–0.37	0.80–1.10	0.025	0.035

Technological conditions of the experiment were chosen based on the catalogue values of milling machine manufacturers. Three cutting speeds, v_{c1} – v_{c3} , one (constant) feed per tooth, f_z , and different depths of cut, a_p , were chosen for the greater explanatory value of the experiment. An overview of cutting conditions for individual milling cutters is given in Tables 4 and 5.

Each of the milling cutters was tested during milling at three cutting speeds $v_c = 100, 125$ and 150 m/min, at constant feed per tooth and various depths of cut. The depths of cut were determined from 5 to 30 mm. It is important to note that the total groove depth for commercial cutters was 20 mm and for newly designed cutters 30 mm. The reason why commercial milling cutters were not tested at higher depths was that after testing several commercial milling cutters, the vibration characteristic time records showed acceleration values above the sensor range throughout the amplitude. Another reason was that the experiment in this first phase was only to verify the correct setting of boundary conditions when recording and evaluating vibrations during milling.

3.4 Measurements and evaluation methodology

3.4.1 Vibration analysis

To keep the machining process safety, reliability and due to avoiding a machine or tool breakage, the monitoring and control of production processes are currently becoming a driving force for the development and sustainability of industries [37]. Technical monitoring methods are traditionally divided into two methods: direct and indirect. Direct methods require the use of vision systems. However, cutting fluid, lighting and others can interfere with the monitoring system and the machine tool, which can lead to an unstable system for the production environment. Nevertheless, some measuring systems have been developed to assess tool wear using laser sensors that measure light shift and intensity. Besides, a combination of cameras can be used simultaneously to capture images of tools during machining. Direct monitoring methods can achieve a high degree of accuracy, but due to many practical limitations, they are characterized as laboratory-oriented techniques. Also, for instance, acoustic emission sensors face certain problems in terms of radio waves and electromagnetic energy. On the other hand, indirect monitoring methods are less accurate but more suitable for practical machine-level applications. Auxiliary quantities are measured and empirically correlated with machining phenomena.

One of the methods of monitoring technical conditions of machines and their components and tools without the equipment disassembling is so-called vibrodiagnostics, which is based on the measurement and analysis of vibration signals. Through the signal processing and its diagnostics, it is possible to identify the errors without operation interruption and to analyse the possible or beginning damage in time that appears as one of the advantages of this method that has recently seen a huge breakthrough in production use. Its application enables a safe and reliable increase in production efficiency; therefore, the authors selected this method for their research.

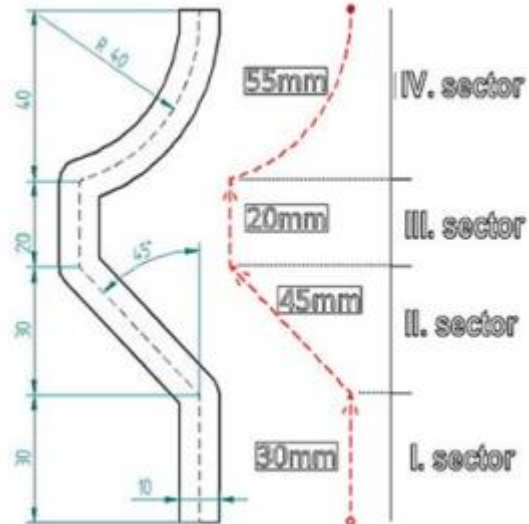
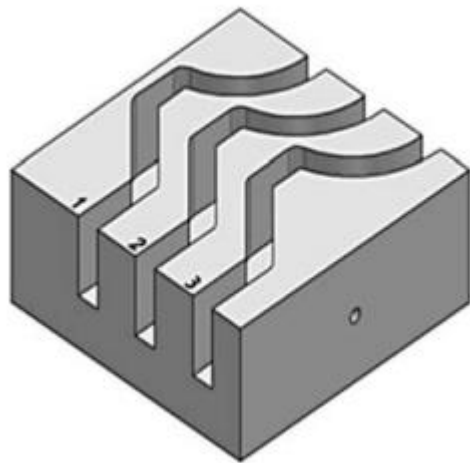


Fig. 4 Three-dimensional model of the workpiece and the groove sizes

Table 4 Cutting conditions of commercially produced milling cutters

Cutter	Procedure	Cutting speed v_c (m/min)	Revolutions per minute n	Feed per tooth f_z (mm/tooth)	Feed per revolution f_n (mm/rev)	Feed v_f (mm/min)	Cutting depth a_p (mm)	Total depth (mm)	Number of transitions
1	Mitsubishi VQMHVD 1000	100	3185	0.04	0.16	510	5	20	4
		125	3981						
		150	4777						
2	HHV 97.016.809	100	3185	0.04	0.16	510	5	20	4
		125	3981						
		150	4777						
3	HHV 98.102.028	100	3185	0.04	0.16	510	5	20	4
		125	3981						
		150	4777						

During the milling of the grooves with the individual milling cutters, the time records of the vibration signals from the three accelerometers were recorded using NI 9234 module and TDG141 recorder with a sample rate of 51.2 kHz. Accelerometers of IMI company were connected to the machine spindle (in the y-axis) and workpieces (in the y and z axes). These are the 607A11 piezoelectric PCB accelerometers with a maximum acceleration range of 50 g. The surfaces for accelerometer connecting were ground in advance; the holes 5 mm in diameter were drilled, and M6 threads were cut to fix them. The connection of the accelerometers through the screws was selected due to an increase of a resonance frequency. The connection to the computer was made via a USB connection. The scheme of measurement is in Fig. 5, and the real view of the connection of accelerometers 1-3 during the experiment is shown in Fig. 6.

All data were analysed using the LabVIEW® software application, where it is possible to create FFT (fast Fourier transformation) spectra and subsequently read RMS values from them. Using Fourier analysis, any waveform in the time domain can be represented by the weighted sum of sine and cosine signals. Using this concept, the FFT spectrum analyser samples the input signal. It then computes the magnitude of its sine and cosine components of the overall signal, and finally, it displays the spectrum

of the signal [38]. RMS is a statistical measure of the magnitude “x” of a varying quantity. This measure gives additional information about the signal, namely the “power” of the signal. First, the value of each point of the signal is squared, then these values are averaged over time, and then once this single number is calculated, the square root of this number is the RMS value of the signal. For discrete data points, this is mathematically calculated through Eq. (6) [39].

$$RMS = \sqrt{\frac{1}{n} (x_1^2 + x_2^2 + \dots + x_n^2)}, \quad (6)$$

where x a magnitude and n is the sequential number of steps in time.

Table 5 Cutting conditions of newly designed milling cutters

Cutter	Indications	Cutting speed v_c (m/min)	Revolutions per minute n	Feed per tooth f_z (mm/tooth)	Feed per revolution f_n (mm/rev)	Feed v_f (mm/min)	Cutting depth a_p (mm)	Total depth (mm)	Number of transitions
1	01-FVT	100	3185	0,04	0,16	510	5	30	6
		125	3981			637	10		3
		150	4777			764	15		2
2	02-FVT	100	3185	0,04	0,16	510	10	30	3
		125	3981			637	15		2
		150	4777			764	30		1
3	03-FVT	100	3185	0,04	0,12	382	10	30	3
		125	3981			478	15		2
		150	4777			573			

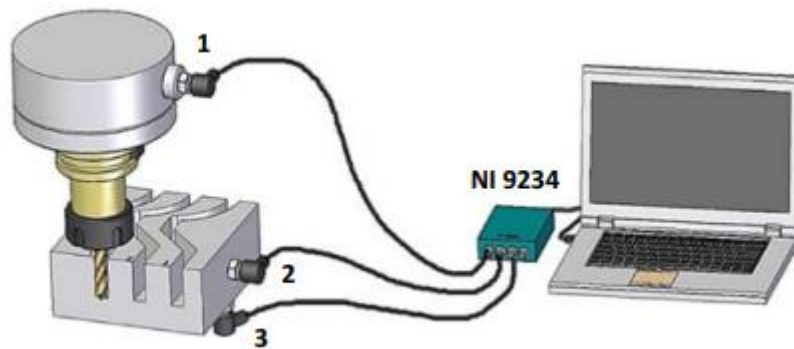


Fig.5 A scheme of measuring set

For continuous functions, it is Eq. (7) [36].

$$RMS = \sqrt{\left[\frac{1}{T} \int_1^T x^2 \right] dt}, \quad (7)$$

where T is the time over which the average is taken.

The main usage of this parameter is to monitor the overall vibration level, and it could be considered as an advantage when compared it with other vibration response parameters, e.g. crest factor (CF) designed to detect early impulses appearing in the signal that is characteristic for an incipient tooth fault or kurtosis designed to react according to the shape of the signal's amplitude distribution [40]. Because of the way RMS in its nature is designed, its value does not increase with increasing the isolated peaks in the signal. Only a periodic series of high energy events will increase the overall level of vibration, hence increasing the value of RMS, so it can be said that it respects the oscillation phenomena more precisely with regard of an expected estimation. As a result, this parameter is easy to evaluate; it is not sensitive to incipient tooth failure and starts indicating a fault only after the tooth damage crossed a certain level of severity. Using the RMS signal during milling, the normal tool characteristics can be distinguished from the abnormal ones.

During the movement of the milling cutter through the individual parts of the trajectory, the vibration characteristic behaviour and its amplitude changed significantly. Due to this reason, the recorded signal was divided into four sections (by sectors I to IV) and each sector was subsequently analysed

separately to be FFT spectra and RMS values influenced at minimum. The procedure for analysing FFT spectra would be a little more complicated than comparing time records since the FFT spectrum from the entire record would contain a large amount of data to be processed. Therefore, for each milling sector I-IV, the "midpoint" of the record was identified (calculated by the feed rate and length of the section), and in this place, the analysis was performed in the range of 10 tool revolutions. A principle of the evaluating method is shown in Fig. 7, and an example of analysed vibrations of commercially produced end mill HHW (operating at three various cutting speeds) is presented in Fig. 8.

The RMS values were recorded from LabVIEW® software application when analysing each cutter, during machining at all cutting speeds, at all depths of cut, at all transitions, at all three sensors, at each groove sector and for each channel separately. That is, four RMS values were read at milling every groove (i.e. one value per sector). An average value for every sector was calculated based on RMS obtained from all transitions of the cutter. These average values were used for plotting bar charts due to comparing the vibrations originated at the machining by individual end mills with different cutting parameters in every sector. Because of a lot of measured data, only these recorded by channel 2 are presented in the article as the most appropriate representative information about the cutters' behaviour.

An example of the effective values recorded by channel 2 at milling with the 01-FVT cutter at cutting speed 100 m/ min is presented in Table 6.

3.4.2 Surface roughness analysis

The evaluation of the surfaces machined by individual milling cutters was carried out based on values of arithmetical average deviation from a mean line, Ra, and maximal height of profile irregularities, Rz. These are the most commonly used parameters for assessing surface roughness. All values were recorded using a Mitutoyo SJ 400 contact equipment. Measurements were made on the first (straight) groove sectors (Fig. 9), and each measurement was repeated four times. The data were statistically processed, while the Grubs test was used for the elimination of gross measurement errors. Subsequently, arithmetic means were calculated and graphical dependencies were processed.

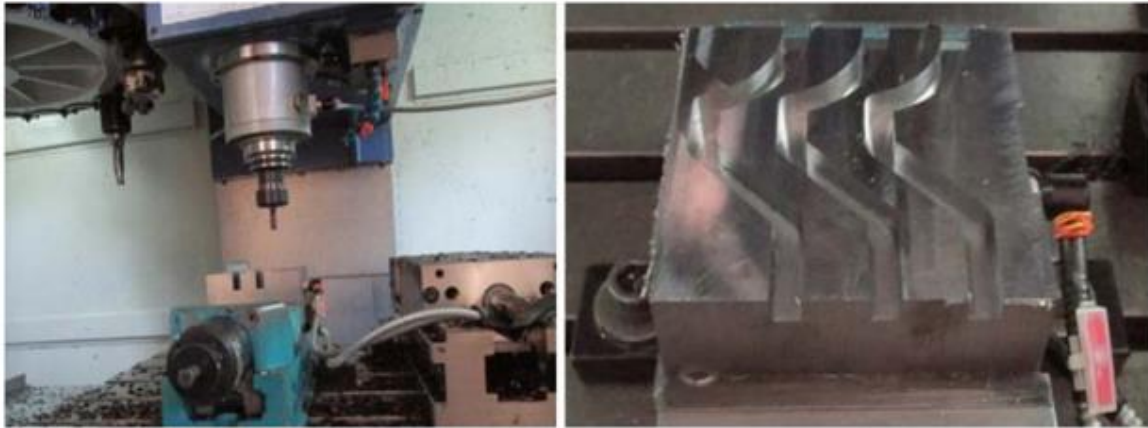


Fig. 6 The experiment preparation and the machined grooves

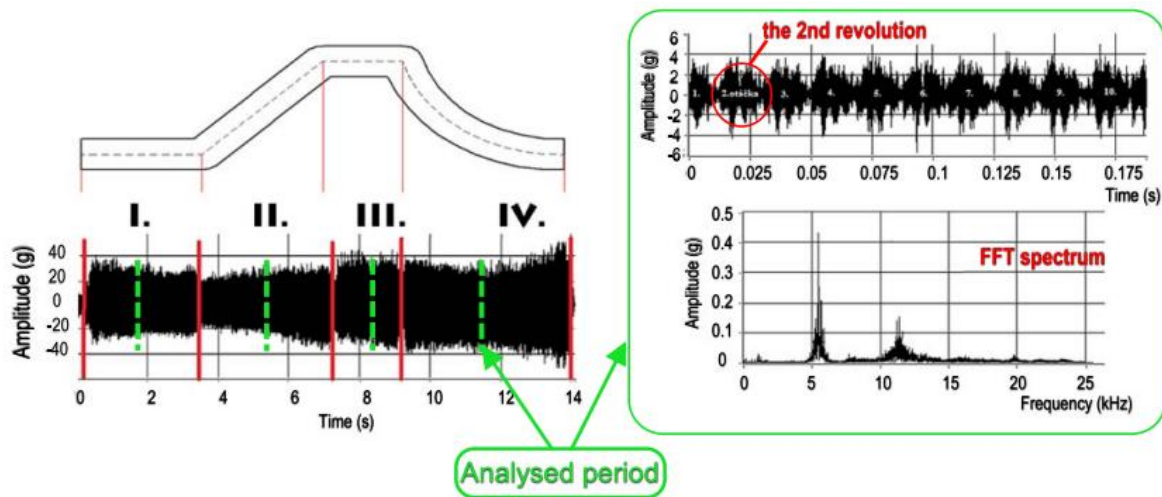


Fig.7 A principle of the evaluating method

4 Results and discussions

In total, more than 250 time records of vibration signals were done. They differ not only in the behaviour but also the amplitude. To show all of them in the presented manuscript would be impossible, so authors decided to present the results through RMS values obtained in individual sectors of the machined groove for every tested milling cutter. Only the records from channel 2 are presented as the representative RMS values reflecting the cutters behaviour at the machining with different cutting parameters. The recording of vibrations in the time domain was performed during machining by all the mentioned milling cutters (3 commercially produced end mills and 3 newly designed by authors) at three different cutting speeds $v_c = 100, 125$ and 150 m/min and different depths of cut. However, it is necessary to notice that acceleration amplitudes of the commercial cutters measured at depths of cut higher than $a_p = 5$ mm were above the sensor range, so only depth of cut 5 mm was selected for experimental testing of commercially produced end mills.

4.1 Evaluation of vibration behaviour of commercially produced end mills

4.1.1 VQMHVD cutter

The analysis of vibration records in the time domain when machining a shaped groove with a commercial VQMHVD cutter showed the lowest acceleration amplitudes at a cutting speed of 150 m/min, at which values did not exceed the range of - 2.5 g to 2.5 g.

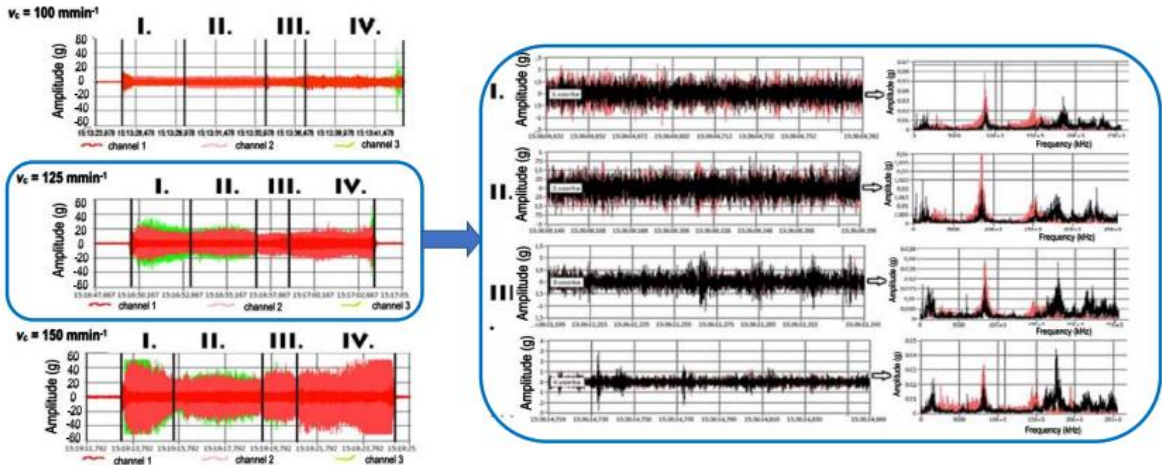


Fig. 8 An example of analysed vibrations of commercially produced end mill HHW

Table 6 An example of the effective values recorded by channel 2 at milling with the O1-FVT cutter (100 m/min)

Cutting depth	RMS values in individual sectors				
	Transition	I.	II.	III.	IV.
$a_p = 10$ mm	First	1.397	1.313	0.968	0.816
	Second	1.317	1.311	0.886	0.998
	Third	1.108	1.474	0.889	0.737
	Average	1.274	1.366	0.914	0.850
$a_p = 15$ mm	First	1.091	1.162	0.696	0.622
	Second	1.188	0.959	0.774	0.512
	Average	1.139	1.060	0.735	0.567

On the other hand, at the lowest speed of 100 m/min, the amplitudes were just below the sensor range, which was why these commercial cutters were not tested at depths of cut higher than 5 mm. Machining at 125 m/min showed amplitudes in the range of - 15 to 15 g.

An analysis of the RMS values (Fig. 10) confirmed that a speed of 150 m/min could be considered to be the most suitable cutting speed for the deep groove milling with a commercial VQMHVD milling cutter since the RMS values were the lowest in all four groove sectors.

4.1.2 HHW cutter

The milling with the commercial HHW cutter also took place only at a depth of cut of 5 mm (the groove was milled to a maximum depth of 20 mm at 4 transitions). The vibration records in time domain showed different amplitude ranges at different milling speeds, while a rate of 100 m/min appeared as the optimal cutting speed for which the amplitude ranges did not exceed - 3 to 3 g.



Fig. 9 Surface roughness measurement device Mitutoyo with detail of the tip

At 150 m/min, variable amplitude values were recorded when the cutter has been passing through the individual groove sectors. The maximum amplitude values at this speed were recorded in sector II, and their values ranged from - 30 to 30 g. The RMS values are shown in Fig. 11, and they correspond to the behaviour of cutters in individual sectors at individual speeds.

4.1.3 HHW BlueCut cutter

The commercial cutter HHW BlueCut operated similarly to the previous HHW cutter under the same cutting conditions, i.e. a 5-mm depth of cut at three different speeds. Although the milling cutter is from the same manufacturer as the milling cutter HHW, the special sodium-cobalt (NaCo) coating and the constant helix angle changed the vibration records at all speeds. The amplitude was tuned at all speeds compared with the HHW mill cutter; however, the lowest acceleration amplitudes (in the range of - 2.8 to 2.8 g) were recorded at 125 m/ min. So, for the HHW BlueCut end mill, the cutting speed of 125 m/min has been identified as the most suitable cutting speed, which was again confirmed by the RMS values shown in Fig. 12.

4.1.4 Evaluation of cutting conditions set-up

By analysing the data of the FFT spectra as well as the RMS values, different optimal cutting speeds were recorded for each milling cutter. For VQMHVD end mill, it was $v_c = 150$ m/min; for HHW, it was $v_c = 100$ m/min, and for HHW BlueCut cutter, it was $v_c = 125$ m/min.

All three commercially produced end mills have been produced from sintered carbide, but they have different helix leads and different coatings. Other conditions were the same when machining the deep grooves with the same technological parameters. Both of these parameters have a big influence on the cutting performance of the end mill. Although only a few papers [41-49] analysed the milling with the inclusion of the effect of the helix angle, all of them confirmed an important role of the helix angle on the instability of cutting process due to repetitive impact-driven chatter and its relation to the cutting forces. Some of them also deal with the influence of helix angle on the mechanism of a chip formation and its removal. Along with findings of the authors above, it can be stated also based on the experiments carried out within the study, that the stability of the machining increases with a higher helix angle because of the most unstable process shows the cutter with smallest helix angle.

The different coatings provide the tool with different properties, such as wear resistance, thermal dissipation or low friction coefficient. The high temperatures that the tools are subjected during milling, over the course of many machining cycles, cause residual stress build-up in the coating, causing cracks (comb cracks) and promoting crack propagation, the latter being the main influencer of the durability of the coated tool.

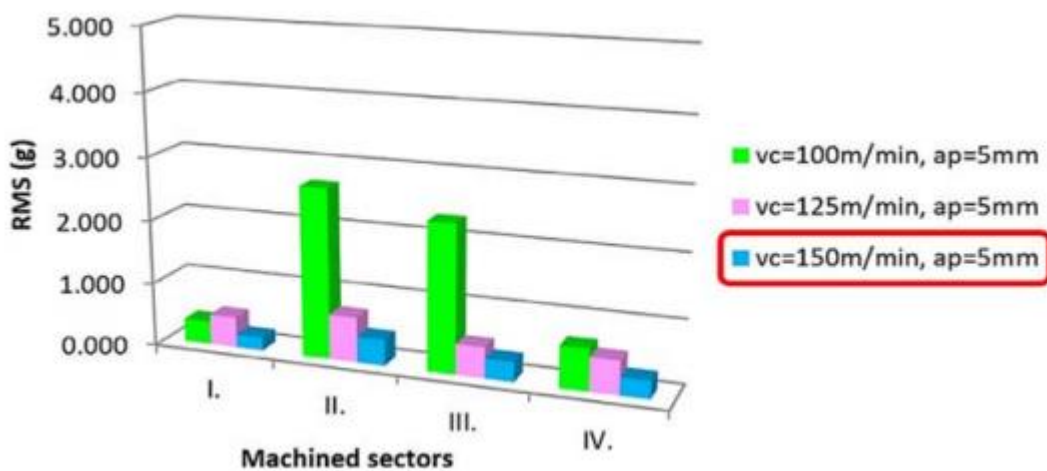


Fig. 10 Time recordings of signals for milling cutter 01 VQMHVD cutter and depth of cut of 5 mm

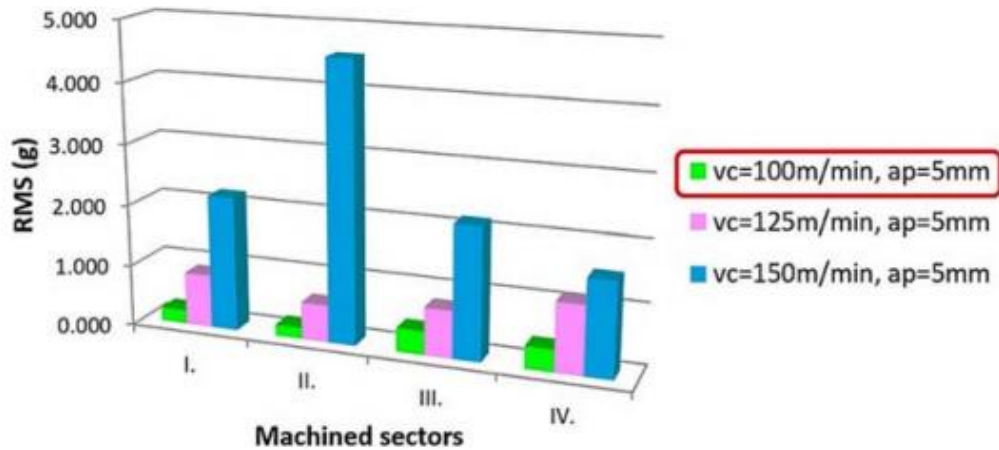


Fig. 11 Time recordings of signals for milling cutter 02 HHW and cutting depth of 5 mm

Residual stresses caused during the coating process also affect the coated tool's machining abilities. The results obtained in this phase of the research also confirmed the knowledge of the other researchers [50-55] that the coating having the highest friction coefficient influence the stability of milling process in a negative way like that has been confirmed by HHW cutter with TiAlN.

However, in every case, the selection of commercially produced milling cutters for the first phase of experiments was done so that all three tools have the different characteristics and their behaviour during the machining was different because of the necessity to recognize the differences at setting up of vibrodiagnostic boundary conditions.

Since the vibrations are closely related to the surface quality, authors decided to verify the results of cutters vibration behaviour also by comparing to the surface roughness achieved after machining with individual commercial cutters. The values of Ra and Rz were measured in every sector of the end mill path five times and after that, they were averaged. The Rz values for the individual investigated cutting speeds are shown in Fig. 13.

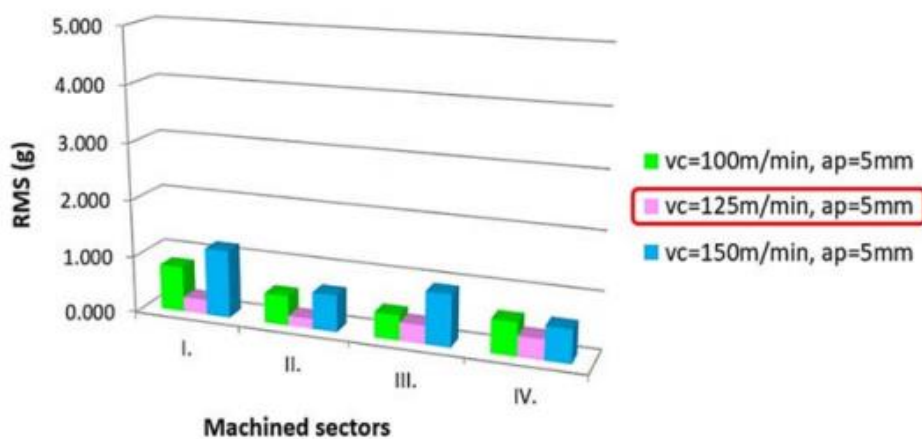


Fig. 12 Time recordings of signals for milling cutter 03 HHW BlueCut and depth of cut of 5 mm

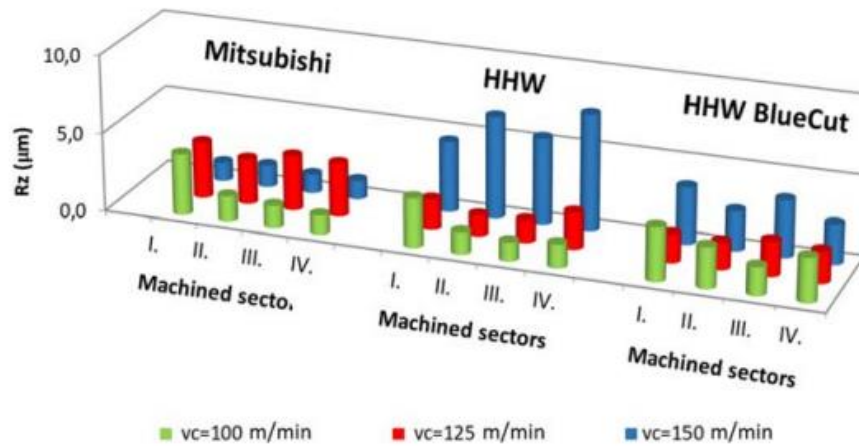


Fig. 13 Surface roughness values R_a after the groove machining with a cutting depth of 5 mm

The graph shows that the lowest surface roughness R_z (in the range 0.8-1 μm) was achieved by VQMHVD tool at 150 m/min cutting speed. At the machining, through HHW end mill the lowest R_z values (0.8-1 μm) were achieved at cutting speed 100 m/min except for the first sector, where higher surface roughness (2.4 μm) was observed than it was at cutting speed 125 m/min. The best surface roughness (in the range 1.2-1.5 μm) was achieved at $v_c = 125$ m/min when milling with the HHW BlueCut (although in the third section, the surface roughness R_z was 2 μm that was worse value by 0.2 μm as compared with the speed of 100 m/min). In terms of comparing the properties of the milling cutters based on R_z , it can be stated that the VQMHVD cutter achieved the best surface of all three commercially produced milling cutters at the highest investigated speed of 150 m/min.

The measured surface roughness confirmed the conclusions of the vibration tests in which the aim was to identify the most suitable cutting conditions of commercially produced milling cutters (in this case the most suitable cutting speed, since the depth of cut was constant). Based on the results achieved in the first phase of the research, it was possible to identify the most suitable cutting conditions for milling cutters designed by the authors.

4.2 Evaluation of newly designed end mills

Groove milling with newly designed cutters 01-FVT, 02-FVT and 03-FVT was carried out under the same conditions as it was with the commercially produced milling cutters; however, the grooving was performed at different depths of cut $a_p = 10$ and 15 mm. Vibrations behaviour was recorded by all three sensors in a time domain, as described in "Vibration analysis" section. This was subsequently processed and evaluated using RMS values. In the next part of the manuscript, due to a large amount of data, only the RMS values that were evaluated for channel no. 2 as the best representative of the course of vibrations during milling.

4.2.1 The 01-FVT cutter

Time records recorded during milling with the 01-FVT cutter at the highest cutting speed (150 m/min) and both examined depths of cut of the 10 mm or 15 mm many times exceeded the given acceleration range of the sensors. The lowest acceleration amplitude values were recorded during machining at a cutting speed of 100 m/min at a depth of cut $a_p = 15$ mm, while maximal acceleration amplitudes ranged from - 7.5 to 7.5 g.

The graphical dependencies of the RMS acceleration values shown in Fig. 14 reflect the vibration analysis results recorded in the time domain for the 01-FVT, when the lowest RMS values were specified for cutting conditions $v_c = 100 \text{ m/min}$ and $a_p = 15 \text{ mm}$.

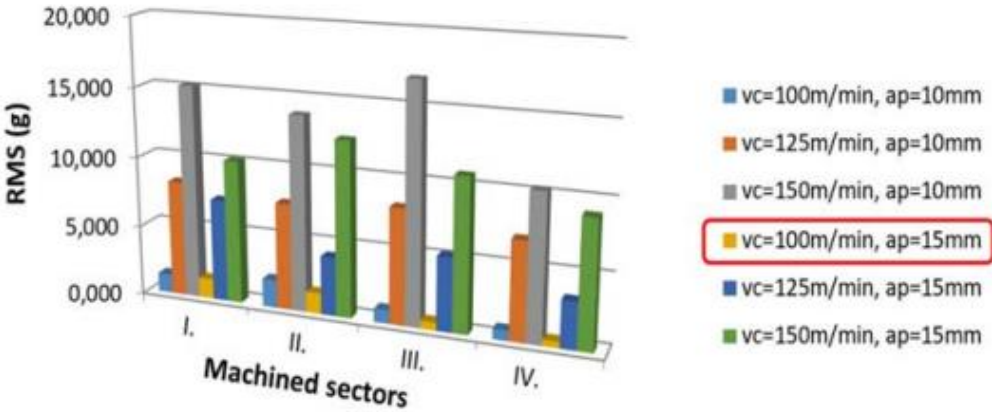


Fig. 14 Dependence of RMS on machining parameters within individual sectors of the groove for cutter 01-FVT

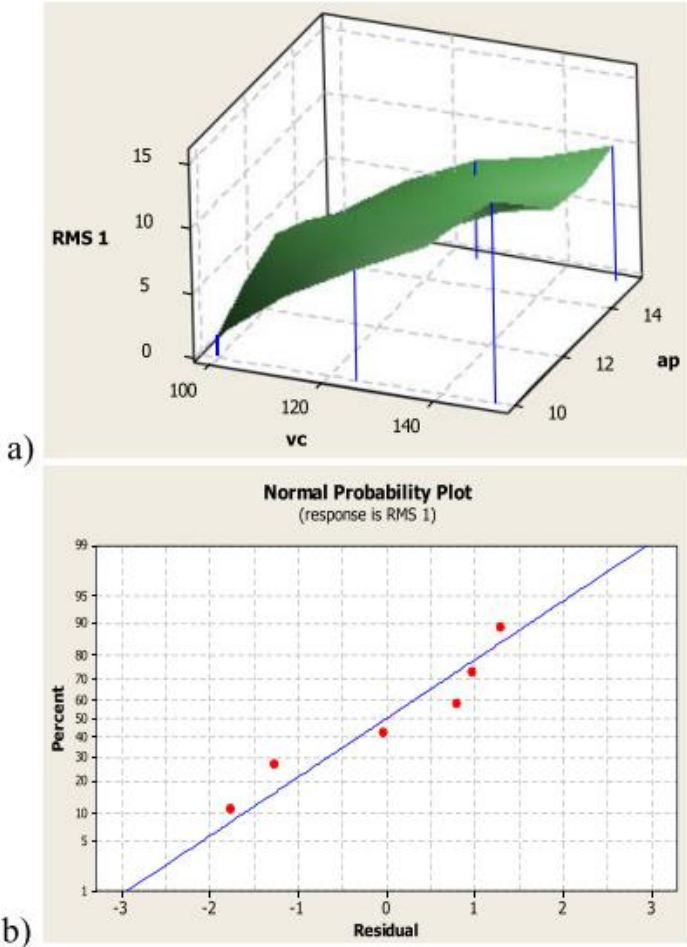


Fig. 15 a Dependency of RMS values on cutting speed and depth of cut within the prediction model for 01 -FVT. b The variance of the measured values relative to the predicted ones

After analysing the effective acceleration values during milling with 01-FVT in the software LabVIEW®, the mathematical prediction model describing the course of RMS values was expressed using Eq. (8) in software MINITAB® 16.2.2, considering the influence of cutting parameters v_c and a_p

$$RMS_{01-FVT} = -16,046 + 0,226v_c - 0,399a_p \quad (8)$$

The correlation coefficient R2 of this linear relation is 95.9%, which means that the equation does not describe only 4.1% of the changes in the examined parameters. The dependency of the RMS values on the cutting speed and depth of cut generated based on the predictive model is shown in Fig. 15a, and the variance of the measured values, relative to the predicted ones, is shown in Fig. 15b.

4.2.2 The 02-FVT cutter

Time record analysis for the 02-FVT cutter showed that even though the cutter has different helix pitch angles to the 01-FVT, only small differences in vibration characteristics were recorded and acceleration amplitudes were within similar maximum ranges. Thus, even in this case, the acceleration amplitude values during machining at the highest cutting speed exceeded the range of accelerometers many times.

A speed of 100 m/min and depth of cut of 10 mm have been evaluated as the best cutting conditions for 02-FVT milling, at which the maximum acceleration amplitude values ranged from - 8.5 to 8.5 g, while at a depth of cut of 15 mm, it was - 16 to 16 g. RMS is in Fig. 16. Comparison of the RMS values with the acceleration values in the time domain for the individual machining parameters confirmed the right selection of the optimum cutting conditions that was done based on vibration records in the time domain.

By analysing the effective acceleration values during milling with the milling cutter 02-FVT using a combination of cutting parameters v_c and a_p , a mathematical predictive model of the vibrator behaviour of the milling cutter concerning cutting speed and depth of cut was expressed.

Since the trend area expressing the predictive behaviour of the 02-FVT milling cutter was curved, it was preferable to create a mathematical model of RMS values initially in logarithmic form through relation (9), and then, using a simple regression in MINITAB® 16.2.2, express the resulting relation (10)

$$\log RMS_{02-FVT} = -9,76 + 4,59 \log v_c + 0,916 \log a_p \quad (9)$$

$$RMS_{02-FVT} = 10^{-9,76} \cdot v_c^{4,59} \cdot a_p^{0,916} \quad (10)$$

The value of the correlation coefficient R2 is 97.2%. The response area of the RMS values depending on the cutting speed and depth of cut is shown in Fig. 17a, and in Fig. 17b is a comparison of predicted and measured RMS values.

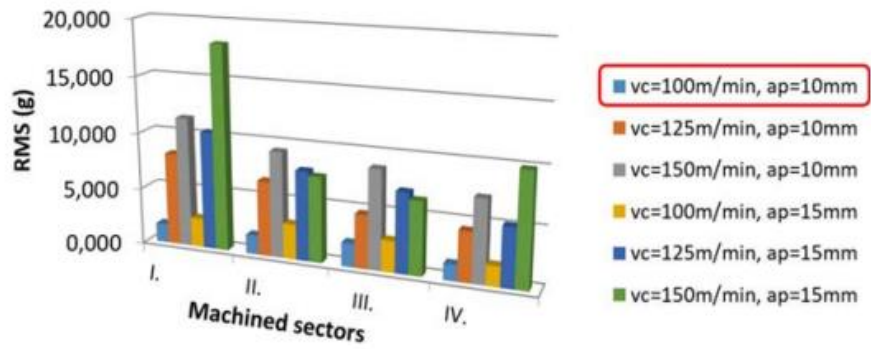


Fig. 16 Dependence of RMS on machining parameters within individual sectors of the groove for cutter 02-FVT

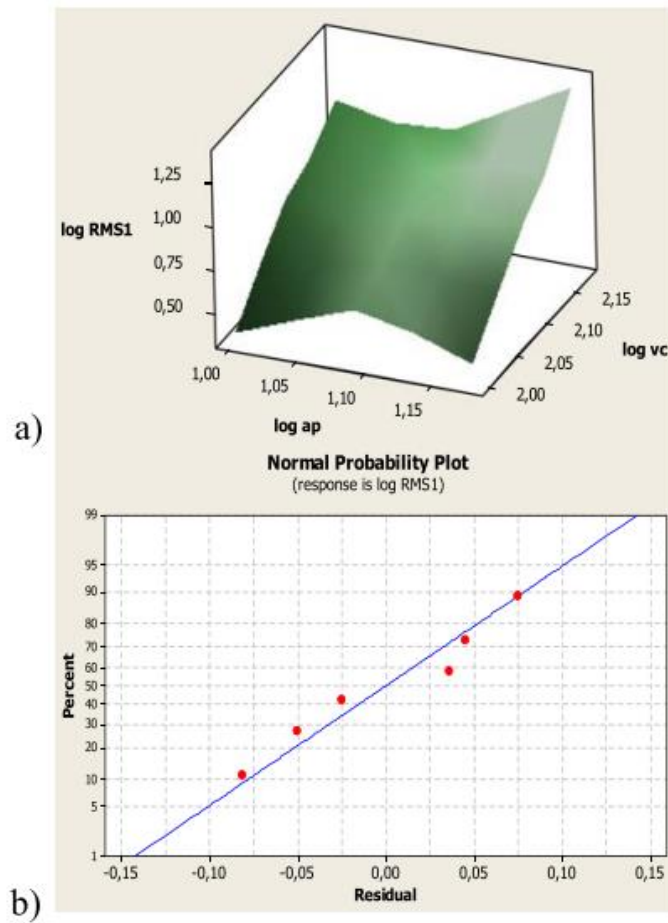


Fig. 17 a) Dependency of RMS values on cutting speed and depth of cut within the prediction model for 02-FVT. b) The variance of the measured values relative to the predicted ones

4.2.3 The 03-FVT cutter

Based on the analysis vibration signals in the time domain during milling with a 03-FVT milling cutter, it can be said that at the maximum cutting speed $v_c = 150$ m/min and the depth of cut of 15 mm, the accelerometer signal values exceeded maximal ranges in all sectors of the groove. Although the acceleration amplitude of milling at a depth of cut of 10 mm did not exceed the maximum sensor range, the amplitude values were very close to the maximum range. At a cut speed of 125 m/min, the amplitude values ranged from -20 to 20 g. Therefore, also for the 03-FVT end mill, the combination of cutting parameters $v_c = 100$ m/min and $a_p = 10$ mm was identified as the most suitable for a given milling cutter and a given type of machining, which was confirmed by the analysis of RMS values (Fig. 18).

Similar to the previous milling cutter, also for the 03-FVT end mill, a predictive model of the milling cutter behaviour with RMS values has been firstly defined by logarithm Eq. (11) created in software MINITAB® 16.2.2. By its further modification into natural coordinates, the dependency of RMS values on cutting speed and depth of cut (12) has been specified.

The correlation coefficient R^2 is 94.8%. Figure 19a has plotted a surface graph of the RMS values as a logarithm function of the cutting speed and the depth of cut, and Fig. 19b shows a comparison of predicted and measured RMS values.

$$\log RMS_{03-FVT} = -11,72 + 5,01 \log v_c + 1,82 \log a_p \quad (11)$$

$$RMS_{03-FVT} = 10^{-11,72} \cdot v_c^{5,01} \cdot a_p^{1,82} \quad (12)$$

4.2.4 Newly designed FVT milling cutters evaluation

When evaluating the behaviour of newly developed milling cutters, it has to be said that the coatings have been the same, but the tools differ in geometry (several characteristics were varied) and in the number of teeth. Therefore, it was difficult to suppose in advance, which of combinations will be the most suitable for the milling of deep grooves. Thus, machining under the same technological conditions (cutting speed and depth of cut) allowed to evaluate the influence of the combination of characteristics on the process stability, or vice versa, at the milling with the same cutter, the best technological parameters could be determined not only in terms of process stability but also from achieved surface roughness. More specifically, the surface roughness analysis has shown that almost all the values were in the range of 0.6-1 ptm with a deviation 6%, when for every combination of the machining conditions and in every sector, the minimum 5 measurements were carried out. So, it can be said that all newly designed cutters are better as for the surface quality achieved after the machining in comparison to the commercially produced end mills.

Since the research was focused on the milling of deep groove, the evaluation was done also from this point of view. By analysing the vibration characteristics, the most suitable machining conditions were specified for each of the newly designed cutters. By their subsequent comparison (Fig. 20) through RMS values, it was possible to conclude that for milling of deep grooves, the 01-FVT cutter will be the most suitable not only due to stability in terms of the lowest RMS values but also because at the same cutting speed the end mill 01-FVT can work most efficiently, i.e. at the greatest depth of cut.

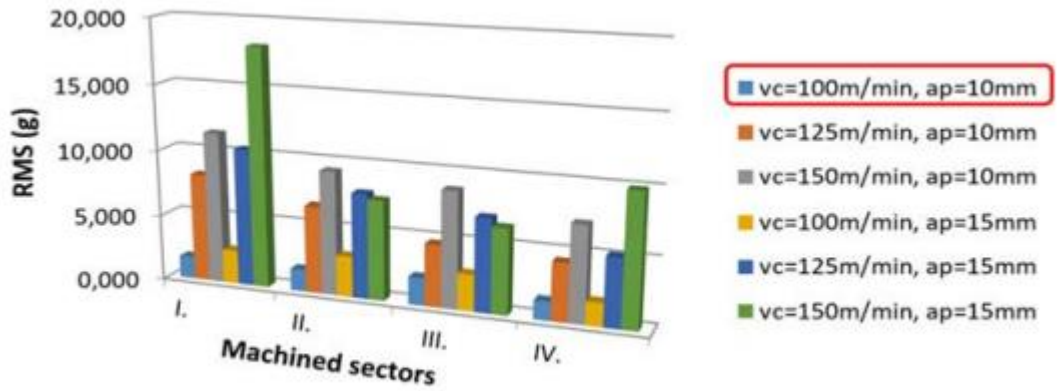


Fig. 18 Dependence of RMS on machining parameters within individual sectors of the groove for cutter 03-FVT

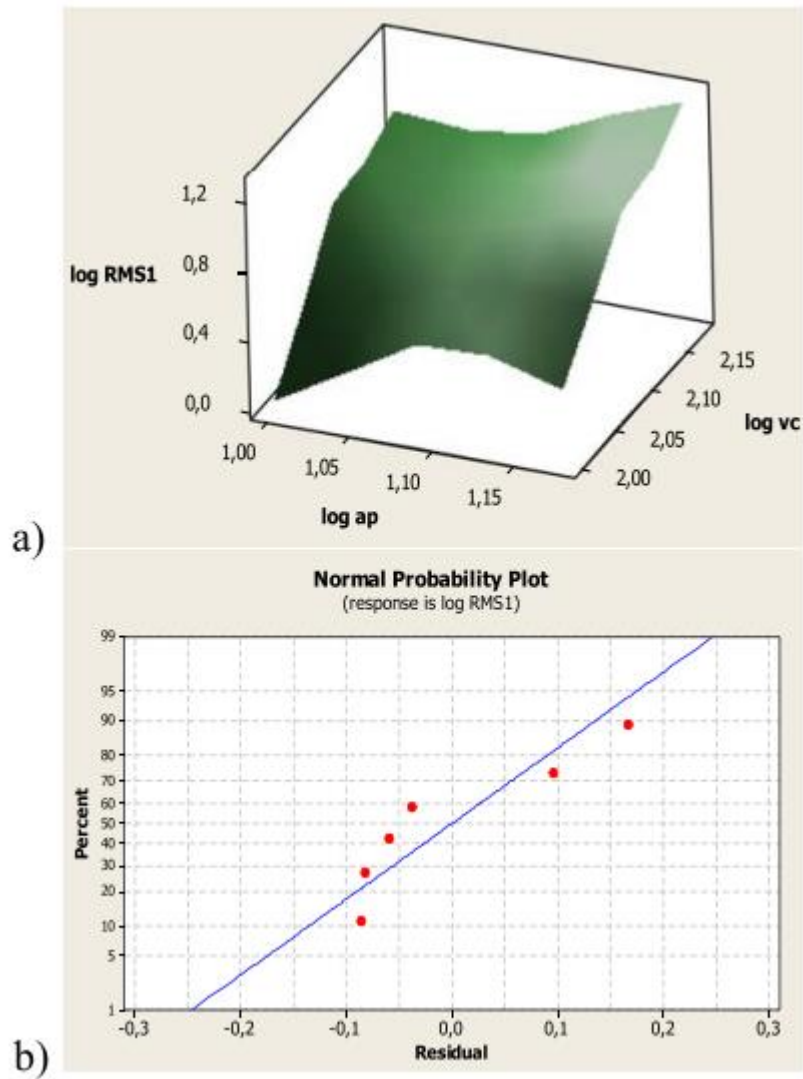


Fig. 19 a Dependency of RMS values on cutting speed and cutting depth within the prediction model for 03-FVT. b The variance of the measured values relative to the predicted ones

Since the research was focused on the milling of deep groove, the evaluation was done also from this point of view. By analysing the vibration characteristics, the most suitable machining conditions were specified for each of the newly designed cutters. By their subsequent comparison (Fig. 20) through RMS values, it was possible to conclude that for milling of deep grooves, the 01-FVT cutter will be the most suitable not only due to stability in terms of the lowest RMS values but also because at the same cutting speed the end mill 01-FVT can work most efficiently, i.e. at the greatest depth of cut.

5 Conclusions

Even today, the technology of metal cutting by milling is one of the most important technologies used for machining various types of surfaces and creating diverse parts. It is therefore important to continue to explore the possibilities of increasing machining efficiency while maintaining or even improving the quality of the manufactured parts [41]. One such option is also pointed out in this article, which deals with increasing machining stability when creating grooves to depths twice as large as the tool diameter through the modifying the geometry of the end mills.

The tool for diagnosing the milling cutters behaviour during experimental testing was vibration analysis. The boundary conditions for the specification of the most suitable machining cutting parameters of newly designed end mills were determined based on vibration diagnostics of the behaviour of commercially produced milling cutters. The conclusions of the vibration tests were verified by surface roughness analysis, in which the values of Ra and Rz were evaluated. Because the amount of measured data was too large, only combinations that have already produced concrete results are listed in the article.

By analysing the FFT spectra and RMS values of commercially produced milling cutters operating at the same depth of cut $a_p = 5$ mm, different optimal cutting speeds were identified for each of the three tested milling cutters. For VQMHVD, it was $v_c = 150$ m/min; for HHW, it was $v_c = 100$ m/min and for HHW BlueCut $v_c = 125$ m/min. The best surface quality in terms of roughness achieved the VQMHVD cutter at cutting speed 150 m/min, the HHW cutter at 100 m/min and the HHW BlueCut at 125 m/min, confirming the use of vibration analysis to identify the best cutting parameters for the new-designed cutters.

Three newly designed milling cutters with different helix angles and different tooth pitches were experimentally tested in the presented paper within the primary goal of the research. All three FVT milling cutters showed the best machining stability at cutting speed $v_c = 100$ m/min, but different depth of cut. The most suitable depth of cut at the machining by the 01-FVT end mill was $a_p = 15$ mm, while for both 02-FVT and 03-FVT end mills, it was $a_p = 10$ mm. For each of the newly designed milling cutters, a mathematical prediction model describing the course of RMS values was developed in MINITAB® software. The surface roughness analysis after machining by newly designed cutters showed that they are better as for the surface quality in comparison to the commercially produced end mills.

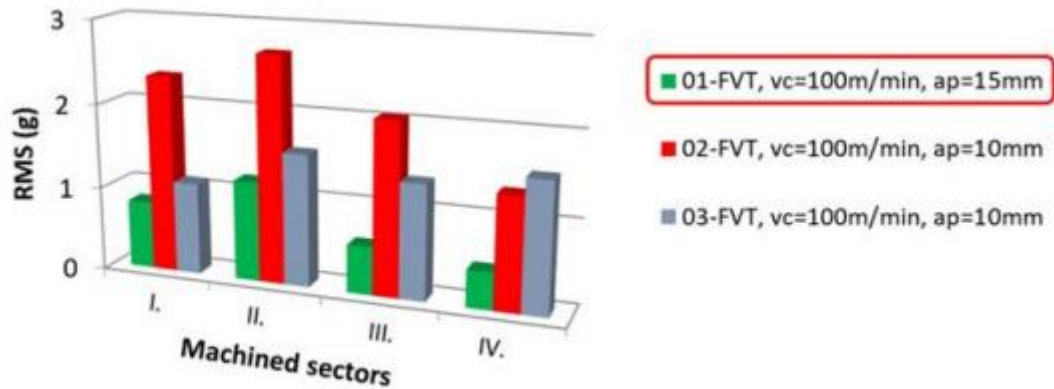


Fig. 20 Comparison of designed cutters under optimal conditions

Finally, it was possible to state that the four-tooth cutter 01-FVT with helix angles ($\beta_1 = 39^\circ$ and $\beta_2 = 41^\circ$) and tooth pitch ($\tau_1 = 83^\circ$ and $\tau_2 = 97^\circ$) seems to be the best tool for milling deep-shaped grooves among all the tested milling cutters. It is not only because of the lowest achieved RMS values but also because, at the same cutting speed, the cutter can work most efficiently, that is, at the highest depth of cut.

It is supposed that the results presented in the article are strongly industrial applicable since the modification of the milling cutters' geometry will bring the effectiveness increasing at the deep grooves milling with the better surface quality achievement in comparison to the commercially produced end mills used for this purpose. The best newly designed milling cutter will be implemented into the real conditions what can result in a financial profit for a company.

References

1. Pimenov DY et al Effect of the relative position of the face milling tool towards the workpiece on machined surface roughness and milling dynamics. *Applied Sciences* 9/5:842
2. Panda A, Prislupčák M, Pandová I (2014) Progressive technology—diagnostic and factors affecting to machinability. *Appl Mech Mater* 616:183-190
3. Baron, P. et al., The parameter correlation of acoustic emission and high-frequency vibrations in the assessment process of the operating state of the technical system, 10/2, 112-116, 2016, The Parameter Correlation of Acoustic Emission and High-Frequency Vibrations in the Assessment Process of the Operating State of the Technical System
4. Stoicovici DI et al (2008) An experimental approach to optimize the screening in the real operating conditions, *manufacturing engineering*, 2. Technical University of Kosice:75-78
5. Kandrak J, Gyani K, Felho C, Deszpoth I (2017) The effect of the shape of chip cross section on cutting force and roughness when increasing feed in face milling. *Manuf Technol* 17:335-342
6. Priyadarshini A, Pal SK, Samantaray AK (2011) A finite element study of chip formation process in orthogonal machining. *Int J Manufact Mater Mech Eng* 1:19-45

7. Monka P, Monkova K, Balara M, Hloch S, Rehor J, Andrej A, Somsak M (2016) Design and experimental study of turning tools with linear cutting edges and comparison to commercial tools. *Int J Adv Manuf Technology* 85:2325-2343
8. Baron P et al (2016) Proposal of the knowledge application environment of calculating operational parameters for conventional machining technology. *Key Eng Mater* 669:95-102
9. Pantazopoulos, G. et al., Accelerated carbide tool wear failure during machining of hot work hardened tool steel: a case study, *international journal of structural integrity*, 6/2, 290-299, 2015, Accelerated carbide tool wear failure during machining of hot work hardened tool steel
10. Mehdi, K., Zghal, A. 2012, Modelling cutting force including thrust and tangential damping in peripheral milling process, *International Journal of Machining and Machinability of Materials (IJMMM)*, 12/3
11. Aydin, M., Koklú, U., A study of ball-end milling forces by finite element model with Lagrangian boundary of orthogonal cutting operation, *Journal of the Faculty of Engineering and Architecture of Gazi University*, 33/2, 507-516, 2018
12. Yong-Hyun K, Sung-Lim K (2002) Development of design and manufacturing technology for end mills in machining hardened steel. *J Mater Process Technol* (130-131):653-661
13. Ali RA et al (2019) Multi-response optimization of face milling performance considering tool path strategies in machining of Al-2024. *Materials* 12:1013
14. Jurko J, Panda A, Behun M (2013) Prediction of a new form of the cutting tool according to achieve the desired surface quality. *Appl Mech Mater* 268-270:473-476
15. Monkova K et al (2019) Comparative study of Chip formation in orthogonal and oblique slow-rate machining of EN 16MnCr5 steel. *Metals* 9:698
16. Sims N; Mann B; Huyanan S., Analytical prediction of chatter stability for variable pitch and variable helix milling tools, *journal of sound and vibration*, 317/3-5, 664-686, 2008
17. Fillipov AV et al (2017) Vibration and acoustic emission monitoring the stability of peakless tool turning: experiment and modeling. *J of Materials Processing Technology* 246:224-234
18. Olvera D, Urbikain G, Elías-Zuniga A, López de Lacalle LN (2018) Improving stability prediction in peripheral milling of Al7075T6. *Appl. Sci.* 8:1316
19. Kim, J. H., Park, J. W., Ko, T. J., End mill design and machining via cutting simulation. *Journal of Materials Processing Technology*, 40/ 3, 324-334, 2008
20. Pantazopoulos GA (2015) Basic principles: some fundamental concepts. *J Fail Anal and Preven* 15:335-336
21. Jerzy J, Kuric I, Grozav S, Ceclan V (2014) Diagnostics of CNC machine tool with R-test system. *Acad J Manuf Eng* 12:56-60
22. Zetek M, Zetkova I (2015) Increasing of the cutting tool efficiency from tool steel by using fluidization method. *Procedia Eng.* 100: 912-917
23. Takuya K, Suzuki N, Hino R, Shamoto E (2013) A novel design method of variable helix cutters to attain robust regeneration suppression. In: *ProcediaCIRP* 8:362-366

24. Grabovski R, Denkena B, Kohler J (2014) Prediction of process forces and stability of end mills with complex geometries, 6th CIRP international conference on high performance cutting. Hannover - Germany, HPC:119-124
25. Wan, M., Yi-Ting, W., et. al.: Prediction of chatter stability for multiple-delay milling system under different cutting force models, International Journal of Machine and Manufacturing 51, China, 281-295, 2001
26. Subramanian, M. et al., Optimization of end mill tool geometry parameters for Al7075-T6 machining operations based on vibration amplitude by response surface methodology, measurement, 46/10, 4005-4022, 2013
27. Sahraoui Z, Mehdi K, Jaber MB (2020) Analytical and experimental stability analysis of AU4G1 thin-walled tubular workpieces in turning process. Proc Inst Mech Eng B J Eng Manuf 234:10071018. <https://doi.org/10.1177/0954405419896115>
28. Vasina M et al (2016) Structural damping of mechanical vibration. Manufacturing Technology 16(6):1379-1382
29. Panda A et al (2016) Evaluation of vibration parameters under machining. Key Eng Mater 669:228-234
30. Al-Zaharnah IT (2006) Suppressing vibrations of machining processes in both feed and radial directions using an optimal control strategy: the case of interrupted cutting. J Mater Process Technol 172:305-310
31. Xiaoliang, J., Chatter stability model of micro-milling with process damping, journal of manufacturing science and engineering, 135/3, 2013
32. Kundrak J, Szabo G, Markopoulos AP (2016) Experimental and numerical investigation of the influence of cutting speed and feed rate on forces in turning of steel. Mater Sci Forum 862:270-277
33. Bagci E (2011) 3-D numerical analysis of orthogonal cutting process via mesh-free method. Int J Phys Sci 6:1267-1282
34. Glaa N, Mehdi K, Moussaoui K, Zitoune R (2020) Numerical and experimental study of the drilling of multi-stacks made of titanium alloy Ti-6Al-4V: interface and burr behaviour. IJAMT 107:11531162. <https://doi.org/10.1007/s00170-020-05116-0>
35. Zorev N N., Inter-relationship between shear processes occurring along tool face and on shear plane in metal cutting[C]. International Research in Production Engineering. New York: ASME,1963, 4249
36. Monkova K, Monka PP, Sekerakova A, Tkac J, Bednarik M, Kovac J, Jahnatek A (2019) Research on chip shear angle and built-up edge of slow-rate machining EN C45 and EN 16MnCr5 steels. Metals 9:956
37. Chryssolouris G, Papakostas N, Mavrikios D (2008) A perspective on manufacturing strategy: produce more with less. CIRP Journal of Manufacturing Science and Technology 1(1):45-52
38. Valicek, J. et al., Analysis of signals obtained from surfaces created by abrasive waterjet by means of amplitude-frequency spectra and autocorrelation function, 15/1, 25-3, 2008
39. Altintas Y (2000) Manufacturing automation—metal cutting mechanics, machine tool vibrations, and CNC design, 1st edn. Cambridge University Press, New York

40. Rzeszucinski PJ, Sinha JK, Edwards R, Starr A, Allen B (2012) Normalised root mean square and amplitude of sidebands of vibration response as tools for gearbox diagnosis. *Strain* 48(6):445-452
41. Zetek, M., Zetkova, I., Influence of the workpiece quality on the cutting tool life when gear wheel are machined, *manufacturing technology*, 17/1, 121-125, 2017